



Full length article

Structure and luminescence properties of Ce^{3+} doped $\text{KBa}_{1-x}(\text{Mg/Zn})_x\text{Y}(\text{BO}_3)_2$ and $\text{K}_{1-y}\text{Na}_y\text{BaY}(\text{BO}_3)_2$ phosphors evolved from cation substitution



Rui Xu, Yujun Liang*, Shiqi Liu, Yingli Zhu, Xingya Wu, Kai Li, Wei Zhou

Engineering Research Center of Nano-Geomaterials of Ministry of Education, China University of Geosciences, Wuhan 430074, People's Republic of China
Faculty of Materials Science and Chemistry, China University of Geosciences, Wuhan 430074, People's Republic of China

ARTICLE INFO

Article history:

Received 8 October 2016

Received in revised form 23 December 2016

Accepted 30 January 2017

Keywords:

Phosphor

Cation substitution

Photoluminescence properties

ABSTRACT

The tunable blue-emitting $\text{KBa}_{1-x}(\text{Mg/Zn})_x\text{Y}_{0.95}(\text{BO}_3)_2:0.05\text{Ce}^{3+}$ and $\text{K}_{1-y}\text{Na}_y\text{BaY}_{0.95}(\text{BO}_3)_2:0.05\text{Ce}^{3+}$ phosphors have been investigated via cation substitution of $\text{Mg}^{2+}/\text{Zn}^{2+}$ for Ba^{2+} and Na^+ for K^+ in $\text{KBaY}(\text{BO}_3)_2$ host. The crystal structures, photoluminescence properties, thermal stability and the effect of $\text{Mg}^{2+}/\text{Zn}^{2+}/\text{Na}^+$ concentration on the luminescence characteristics were investigated in detail. The XRD analysis implied that $\text{KBa}_{1-x}(\text{Mg/Zn})_x\text{Y}(\text{BO}_3)_2$ solid solutions were limited, while continuous solid solution was possible in $\text{K}_{1-y}\text{Na}_y\text{BaY}(\text{BO}_3)_2$ system. Upon the excitation at 365 nm, the emission peaks of $\text{KBa}_{1-x}(\text{Mg/Zn})_x\text{Y}_{0.95}(\text{BO}_3)_2:0.05\text{Ce}^{3+}$ ($0 \leq x \leq 0.6$) blue-shifted from 435 to 424 nm, and $\text{K}_{1-y}\text{Na}_y\text{BaY}_{0.95}(\text{BO}_3)_2:0.05\text{Ce}^{3+}$ ($0 \leq y \leq 1$) blue-shifted from 435 to 427 nm with the $\text{Mg}^{2+}/\text{Zn}^{2+}/\text{Na}^+$ doping concentration increase. The thermal stabilities of $\text{KBa}_{1-x}(\text{Mg/Zn})_x\text{Y}_{0.95}(\text{BO}_3)_2:0.05\text{Ce}^{3+}$ phosphors were enhanced from 20 °C to 200 °C by increasing the concentration of Mg^{2+} and Zn^{2+} . The substitution of Na^+ for K^+ led to a decrease in the proportion of $^5\text{D}_{5/2}-^7\text{F}_{5/2}$ and $^5\text{D}_{7/2}-^7\text{F}_{7/2}$ corresponding to the Gaussian fitting of Ce^{3+} in $\text{K}_{1-y}\text{Na}_y\text{BaY}_{0.95}(\text{BO}_3)_2:0.05\text{Ce}^{3+}$ phosphors. At the temperature increased, the full width at half maximum of photoluminescence band of $\text{K}_{0.8}\text{Na}_{0.2}\text{BaY}_{0.95}(\text{BO}_3)_2:0.05\text{Ce}^{3+}$ decreased. However, the decreasing trend of FWHM became less obvious with the increasing concentration of Na^+ in the temperature dependent photoluminescence spectra of $\text{K}_{1-y}\text{Na}_y\text{BaY}_{0.95}(\text{BO}_3)_2:0.05\text{Ce}^{3+}$ phosphors.

© 2017 Elsevier Ltd. All rights reserved.

1. Introduction

With the development of solid state lighting, the search and improvement of thermally stable, highly efficient phosphors with suitable excitation and emission wavelengths have been attracting more attention than ever [1–4]. Nowadays, in order to acquire better performing phosphors, tuning the crystal field environment of activator in the host lattice is the main trend [5–7]. The solid solution design strategy is an efficient way to tune the crystal field environment with diverse compositions. Compared with the combinatorial chemistry screening [8], or the single-particle-diagnosis approach [9,10], the strategy of solid solution design approach gets rid of massive preparation of phosphor library, making composition design more targeted. The solid solution phosphor always presents predictable luminescence properties, making it more reliable to achieve desired parameters. Commonly it processes in two dif-

ferent manners, the chemical unit substitution or the cation/anion substitution. Recently, the effect of cation substitution in phosphors has been experimentally analyzed by many reports. For instance, Wang et al. reported that the emission peaks of $\text{Ba}_{(3-x)}\text{Sr}_x\text{Lu}(\text{PO}_4)_3:\text{Eu}^{2+}$ ($0 \leq x \leq 3$) phosphors were blue-shifted, from 506 to 479 nm, with increasing Sr/Ba ratio upon the same excitation wavelength of 365 nm [11]. Bulloni et al. found that the substitution of Ca^{2+} for Sr^{2+} in the $\text{Sr}_2\text{Si}_5\text{N}_8$ host lattice provoked a red-shifting of the emission peak of Eu^{2+} , from 620 nm to 643 nm [12]. And Yu et al. discovered that the red-shift from 540 nm to 556 nm with increasing Gd/La ratio in solid solution phosphor, $(\text{La,Gd})\text{Sr}_2\text{AlO}_5:\text{Ce}^{3+}$ [13].

In recent years, rare earth doped borate phosphors have attracted great attention due to the advantages of high luminescence efficiency, better color purity and excellent product performance. The different borate phosphors doped by rare earth ions have been reported with good photoluminescence properties [14–17]. Among them, a buetschliite-type rare-earth borate $\text{KBaY}(\text{BO}_3)_2$ (KBYP), which was first synthesized by Gao et al., was considered [14]. It was reported that the phosphors crystallize in the

* Corresponding author at: Faculty of Materials Science and Chemistry, China University of Geosciences, Wuhan 430074, China.

E-mail address: yujunliang@sohu.com (Y. Liang).

trigonal space group R-3m. In order to tune the color of the borate species, many researchers doped other rare earth ions or alkaline-earth metal ions into this host and some successful experiments have been reported [15–17]. Wang's group observed the efficient energy transfer from the host to Tb^{3+} in $\text{KBYB}:\text{Tb}^{3+}$ phosphor [15]. Then, Lian et al. investigated that $\text{KBYB}:\text{Ce}^{3+}$, Mn^{2+} and $\text{KBYB}:\text{Ce}^{3+}$, Tb^{3+} could be two promising single-phased phosphors for n-UV white-light emitting diodes [16,17]. Zhang et al. synthesized and reported that Ce^{3+} , Tb^{3+} , Eu^{3+} tridoped KBYB phosphors exhibited broadband NUV absorption and blue-green-red tunable emission, which might serve as down-converted phosphors for NUV light-emitting diodes [18]. However, the effect of substituted ions on the crystal structures, PL properties and thermal stabilities of $\text{KBYB}:\text{Ce}^{3+}$ phosphor did not receive much attention.

In this study, we used the solid solution design way to evaluate the effects of cation substitution Mg^{2+} or Zn^{2+} for Ba^{2+} and Na^{+} for K^{+} in $\text{KBYB}:\text{Ce}^{3+}$. The crystal structures, photoluminescence properties and thermal stability of $\text{KBa}_{1-x}(\text{Mg}/\text{Zn})_x\text{Y}_{0.95}(\text{BO}_3)_2:0.05\text{Ce}^{3+}$ and $\text{K}_{1-y}\text{Na}_y\text{BaY}_{0.95}(\text{BO}_3)_2:0.05\text{Ce}^{3+}$ phosphors with increasing concentration of Mg^{2+} , Zn^{2+} or Na^{+} were discussed. The changes of emission intensity and spectral position of emission peak were considered. The mechanism of the blue-shift and effect of cation substitution on the thermal stability of the phosphors were investigated. The relations between variation of the crystal structure and the Ce^{3+} emission and control of the photoluminescence properties would be of interest for the discovery of new phosphors and tailoring their emission behavior.

2. Experimental

2.1. Materials and synthesis

The designed $\text{KBa}_{1-x}(\text{Mg}/\text{Zn})_x\text{Y}_{0.95}(\text{BO}_3)_2:0.05\text{Ce}^{3+}$ ($x = 0, 0.1, 0.2, 0.3, 0.4, 0.5, 0.6$) and $\text{K}_{1-y}\text{Na}_y\text{BaY}_{0.95}(\text{BO}_3)_2:0.05\text{Ce}^{3+}$ ($y = 0, 0.2, 0.4, 0.6, 0.8, 1.0$) phosphors were synthesized by a conventional high temperature solid-state reaction. Stoichiometric amounts of K_2CO_3 (99.99%), BaCO_3 (99.99%), MgCO_3 (99.99%), ZnCO_3 (99.99%), Na_2CO_3 (99.99%), H_3BO_3 (99.99%) (Sinopharm Chemical Reagent CO., LTD), CeO_2 (99.99%) and Y_2O_3 (99.99%) (Deqing XingBang Rare Earth New Materials CO., LTD) were weighed and grounded thoroughly in an agate mortar. In each sample, 5 wt% H_3BO_3 (99.99%) was added as a flux. Then, the as-obtained reactant mixture was placed into an alumina crucible and sintered at 950 °C for 6 h in weak H_2 reducing atmosphere. Finally, the prepared phosphors were cooled to room temperature and reground for further measurements.

2.2. Characterization

The phase compositions were characterized by X-ray powder diffraction (XRD) (Bruker D8 Focus, Bruker, Kalsruhe, Germany) with Ni-filtered $\text{Cu K}\alpha$ ($\lambda = 1.540598 \text{ \AA}$) radiation at 40 kV tube voltage and 40 mA tube current. The scanning rate for phase identification was fixed at $12^\circ \text{ min}^{-1}$ with 2θ range from 10° to 70° . Excitation and emission spectra were measured at room temperature by fluorescence spectrometer (Fluoromax-4P, Horiba Jobin Yvon, NJ, U.S.A.) equipped with a 150 W xenon lamp as the excitation source.

3. Results and discussion

3.1. Crystal structure description and phase structure analysis

A representative structure of KBYB is shown in Fig. 1. The powder sample of $\text{KBaY}(\text{BO}_3)_2$ was crystallized in trigonal symmetry

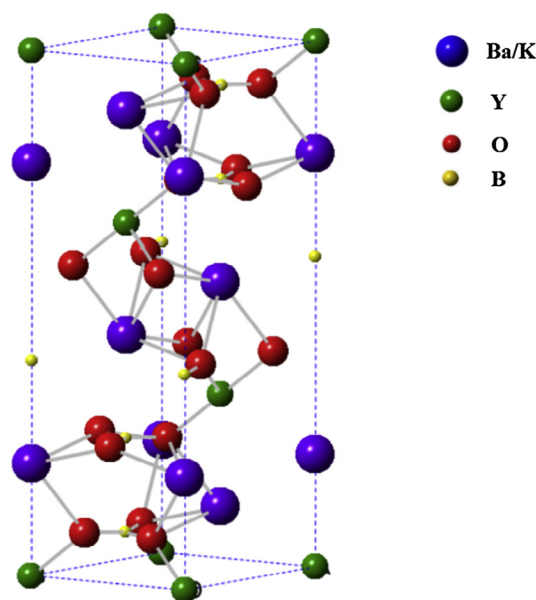


Fig. 1. The structure of $\text{KBaY}(\text{BO}_3)_2$.

with space group R-3m. The lattice parameters were $a = 5.4526(12) \text{ \AA}$, $c = 17.781(8) \text{ \AA}$, $V = 457.8(3) \text{ \AA}^3$ [15]. $\text{KBaY}(\text{BO}_3)_2$ was isotypic with the mineral buetschliite, $\text{K}_2\text{Ca}(\text{CO}_3)_2$ [19,20]. And the crystal structure of KBYB was drawn using CrystalMaker software and shown in Fig. 2a. In the crystal structure of $\text{KBaY}(\text{BO}_3)_2$, the BO_3 triangles and the YO_6 octahedra were linked together by sharing the common oxygen vertices to generate a two-dimensional $[\text{YB}_2\text{O}_6]_\infty$ double layer. There were two crystallographically independent cation sites, namely, one Y^{3+} and one $\text{Ba}^{2+}/\text{K}^{+}$ site, where the Ba^{2+} and K^{+} shared the same site [14]. Y^{3+} was coordinated by 6 O to form slightly distorted octahedron, while the $\text{Ba}^{2+}/\text{K}^{+}$ mixed ion was surrounded by 9 O, as shown in Fig. 2b. From the valence and the ionic radius of Y^{3+} (0.9 Å for coordinate number CN = 6) and Ce^{3+} (1.01 Å for CN = 6) [21], we proposed that Ce^{3+} substituted the Y^{3+} site.

The XRD patterns of the as-synthesized $\text{KBa}_{1-x}(\text{Mg}/\text{Zn})_x\text{Y}_{0.95}(\text{BO}_3)_2:0.05\text{Ce}^{3+}$ and $\text{K}_{1-y}\text{Na}_y\text{BaY}_{0.95}(\text{BO}_3)_2:0.05\text{Ce}^{3+}$ phosphors are shown in Figs. 3 and 4, respectively. As can be seen from Fig. 3a, the impurity phase YBO_3 appeared when Mg^{2+} concentration was 0.6. The results of $\text{K}(\text{Ba}_{1-x}\text{Zn}_x)\text{Y}_{0.95}(\text{BO}_3)_2:0.05\text{Ce}^{3+}$ ($x = 0.1-0.6$) and $\text{K}(\text{Ba}_{1-x}\text{Mg}_x)\text{Y}_{0.95}(\text{BO}_3)_2:0.05\text{Ce}^{3+}$ ($x = 0.1-0.6$) were similar, as illustrated in Fig. 3b. As can be observed in Fig. 4a, K^{+} ions can be substituted completely by Na^{+} ions and the XRD patterns were almost the same from $\text{KBaY}(\text{BO}_3)_2$ to $\text{NaBaY}(\text{BO}_3)_2$. As shown in Fig. 4b, the characteristic diffraction peak shifted to higher angles

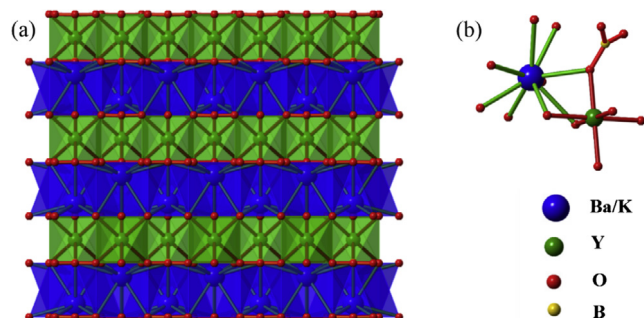


Fig. 2. (a) Crystal structure of $\text{KBaY}(\text{BO}_3)_2$; (b) crystal structure emphasizing the coordination of $\text{Ba}^{2+}/\text{K}^{+}$ and Y^{3+} .

Download English Version:

<https://daneshyari.com/en/article/5007550>

Download Persian Version:

<https://daneshyari.com/article/5007550>

[Daneshyari.com](https://daneshyari.com)